

## **EM-21 Higher Waste Loading Glasses for Enhanced DOE High-Level Waste Melter Throughput Studies - 10194**

Fabienne C. Raszewski, Thomas B. Edwards and David K. Peeler  
Savannah River National Laboratory, Aiken, South Carolina 29808

### **ABSTRACT**

Supplemental validation data have been generated that will be used to determine the applicability of the current Defense Waste Processing Facility (DWPF) liquidus temperature ( $T_L$ ) model to expanded DWPF glass regions of interest based on higher waste loadings. For those study glasses which had very close compositional overlap with the model development and/or model validation ranges (except  $TiO_2$  and  $MgO$  concentrations), there was very little difference in the predicted and measured  $T_L$  values, even though the  $TiO_2$  contents were above the 2 wt% upper concentration covered by the model. The results indicate that the current  $T_L$  model is applicable in these compositional regions. As the compositional overlap between the model validation ranges diverged from the target glass compositions, the  $T_L$  data suggest that the model under-predicted the measured values. These discrepancies imply that the influence of individual oxides or their combinations at concentrations outside of the model development and/or previous validation regions may not be adequately assessed by the current model. These oxides include  $B_2O_3$ ,  $SiO_2$ ,  $MnO$ ,  $TiO_2$  and/or their combinations. More data are required to fill in these anticipated DWPF compositional regions so that the model coefficients could be refit to account for these influences.

### **INTRODUCTION**

High-level waste (HLW) throughput (i.e., the amount of waste processed per unit time) is a function of several parameters, two of which are extremely critical: waste loading (WL) and melt rate. For the Defense Waste Processing Facility (DWPF) at the Savannah River Site (SRS), increasing HLW throughput would significantly reduce the overall mission life cycle costs for the Department of Energy (DOE).

Significant increases in waste throughput have been achieved at DWPF for Sludge Batch 3 (SB3) and Sludge Batch 4 (SB4). Key technical and operational initiatives that supported increased waste throughput included improvements in facility attainment, the Chemical Processing Cell (CPC) flowsheet, process control models and frit formulations [1,2]. As a result of these key initiatives, DWPF increased WLs from a nominal 28% for Sludge Batch 2 (SB2) to ~38% for SB3 while maintaining or slightly improving canister fill times. Although considerable improvements in waste throughput were accomplished, process control models allowed DWPF to target even higher WLs (i.e., 40% and greater), implying that additional improvement in waste throughput could be achieved. Actual facility data have shown that melt rate is significantly reduced at higher WLs, thus adversely impacting waste throughput. Based on these trends, DWPF has elected to target an intermediate waste loading to optimize waste throughput.

Alternative strategies [3] could allow DWPF to achieve higher WLs (45-55%), while minimizing or eliminating the negative impacts on melt rate. WL targets at DWPF could then be limited by current process control model predictions rather than melt rate or waste throughput. In this scenario, there would be a need to identify any conservatism in the current process control

models and, if necessary, generate data in new compositional regions over which the current models were not formally developed.

The current DWPF liquidus temperature<sup>1</sup> ( $T_L$ ) model was first developed over compositions specific to SRS and then later validated with data from the Pacific Northwest National Laboratory (PNNL). Specifically, the DWPF  $T_L$  model was found to adequately predict glasses from a broader compositional region than that for which it was originally developed. Table I contains the oxide ranges used to develop and validate the current  $T_L$  model [4].

Table I. Liquidus Temperature Model Development and Validation Oxide Ranges (wt%).

Oxide	Model Development Range	Model Validation Range
Al <sub>2</sub> O <sub>3</sub>	0.99 - 14.16	0.00 - 16.73
B <sub>2</sub> O <sub>3</sub>	4.89 - 12.65	0.00 - 19.99
CaO	0.31 - 2.01	0.00 - 10.30
Cr <sub>2</sub> O <sub>3</sub>	0.00 - 0.30	0.00 - 1.20
FeO	0.02 - 6.90	0.02 - 6.90
Fe <sub>2</sub> O <sub>3</sub>	3.43 - 16.98	3.43 - 16.98
K <sub>2</sub> O	0.00 - 3.89	0.00 - 4.00
Li <sub>2</sub> O	2.49 - 6.16	0.00 - 7.49
MgO	0.47 - 2.65	0.00 - 7.31
MnO	0.74 - 3.25	0.00 - 4.00
Na <sub>2</sub> O	5.99 - 14.90	4.99 - 22.74
NiO	0.04 - 3.05	0.00 - 3.05
SiO <sub>2</sub>	41.80 - 58.23	29.97 - 58.23
TiO <sub>2</sub>	0.00 - 1.85	0.00 - 5.003

Although validated through the use of existing PNNL data, it is possible that there are compositional gaps (beyond the model *development* ranges) over which the current model has not been validated. These compositional gaps may be a result of several factors:

- Combinations of oxides not covered by the validation data
- Higher waste loadings that increase specific oxide concentrations above those of the validation data
  - For example, Fe<sub>2</sub>O<sub>3</sub>, MnO, Cr<sub>2</sub>O<sub>3</sub> and NiO - all of which can have a significant impact on  $T_L$
- Increased TiO<sub>2</sub> concentrations due to coupled operations (addition of the Monosodium Titanate (MST) stream that is used to remove actinides from the salt waste stream)
- Increased Al<sub>2</sub>O<sub>3</sub> concentrations as higher Al-based waste streams are considered

As a specific example, projections of future sludge batches suggest that the TiO<sub>2</sub> concentrations during coupled operations could be on the order of 5-6 wt% based on Salt Waste Processing Facility (SWPF) high output operations. The current  $T_L$  model was developed using glasses containing a maximum of approximately 2 wt% TiO<sub>2</sub> and has been validated with certain compositions up to 5 wt%; however, the glasses used for validation may not necessarily cover

<sup>1</sup>  $T_L$  is defined as the maximum temperature at which equilibrium exists between molten glass and the primary crystalline phase.

the anticipated DWPF glass region of interest. Another example of a potential mismatch between the compositional region over which models were developed and future DWPF operations is based on the intent of DOE to accelerate the cleanup mission by targeting higher WL glasses (45-55%). As previously mentioned, future sludge compositions and higher WLs may increase the concentrations of some of the sludge components (e.g., Fe<sub>2</sub>O<sub>3</sub>, MnO, Cr<sub>2</sub>O<sub>3</sub>, NiO, and/or Al<sub>2</sub>O<sub>3</sub> etc.) in glass above the maximum values over which the model was developed and/or lead to compositional combinations that extend beyond the validation regions of the current T<sub>L</sub> model.

Regardless of the scenario, additional data are needed to assess the applicability of the current T<sub>L</sub> model at higher TiO<sub>2</sub> concentrations. Additional T<sub>L</sub> data could extend the compositional region over which the current T<sub>L</sub> model is applicable and identify compositional regions outside of the model development region in which the current T<sub>L</sub> model is not applicable. In this case the new data could be used to adjust the empirically-estimated coefficients by refitting the model, if necessary.

The objective of this study is to generate supplemental validation data that could be used to determine the applicability of the current DWPF T<sub>L</sub> model to expanded DWPF glass regions of interest based on higher WLs. Two specific flowsheets were used in this study to provide such insight:

- Higher WL glasses (45 and 50%) based on future sludge batches that have (and have not) undergone the Al-dissolution process
- Coupled operations supported by SWPF, which increases the TiO<sub>2</sub> concentration in glass above 2 wt%

Glasses were also selected to address technical issues associated with Al<sub>2</sub>O<sub>3</sub> solubility and nepheline formation.

## EXPERIMENTAL PROCEDURES

A test matrix of 22 non-radioactive glasses was developed using various frit compositions and five different sludge compositions [5-8]. The terminologies used for sludge types are defined as follows:

1. Cluster 2 avg - representing, in general, future sludge batch projections without Al-dissolution
2. Cluster 4 avg - representing, in general, future sludge batch projections with Al-dissolution
3. MSP-001/SB8 - Coupled operations using the Sludge Batch 8 projection
4. MSP-001/SB9 - Coupled operations using the Sludge Batch 9 projection
5. WOALD-SB19 – Sludge Batch 19 projection that has the highest Al<sub>2</sub>O<sub>3</sub> content (without Al-dissolution)

The glass identification (ID), frit composition, WL and ranges of the major oxides are given in Table II.

Table II. Glass Composition Ranges.

Sludge	Cluster 2 avg	Cluster 4 avg	MSP-001 / SB8	MSP-001 / SB9	WOALD - SB19
--------	---------------	---------------	---------------	---------------	--------------

Frit <sup>a</sup>	A,B	A,C	B,D	D,E	B
WL (%)	45-50	45-50	35-45	32-42	50-55
Glass ID	HWL-01:04	HWL-05:08	HWL-09:14	HWL-15:20	HWL-21:22
Al <sub>2</sub> O <sub>3</sub>	10.8 - 12.1	6.8 - 7.6	4.5 - 5.8	3.8 - 5.1	17.2 - 18.9
B <sub>2</sub> O <sub>3</sub>	7.3 - 10.3	4.7 - 8.0	4.5 - 11.9	4.7 - 12.4	8.1 - 9.0
CaO	1.2 - 1.4	1.5 - 1.7	0.9 - 1.1	0.9 - 1.2	1.4 - 1.6
Fe <sub>2</sub> O <sub>3</sub>	14.4 - 16.1	16.4 - 18.3	10.4 - 13.4	10.7 - 14.1	9.4 - 10.3
Li <sub>2</sub> O	4.2 - 5.1	4.7 - 5.1	4.5 - 5.3	3.5 - 5.5	3.6 - 4.0
MnO	1.9 - 2.1	2.4 - 2.7	3.4 - 4.3	2.3 - 3.0	0.9 - 1.0
Na <sub>2</sub> O	10.0 - 11.1	10.5 - 13.1	8.0 - 13.9	7.5 - 13.7	14.5 - 15.8
SiO <sub>2</sub>	39.9 - 45.0	43.3 - 46.9	43.6 - 52.3	46.4 - 53.3	37.5 - 40.7
TiO <sub>2</sub>	1.5 - 1.7	1.3 - 1.4	2.3 - 3.0	2.7 - 3.6	1.6 - 1.7
Others <sup>b</sup>	1.9 - 2.2	2.2 - 2.5	3.1 - 4.0	2.2 - 3.0	1.3 - 1.4

<sup>a</sup> Compositions for the frits (wt%) are as follows: (A) 14B<sub>2</sub>O<sub>3</sub>-9Li<sub>2</sub>O-1Na<sub>2</sub>O-76SiO<sub>2</sub>, (B) 18B<sub>2</sub>O<sub>3</sub>-8Li<sub>2</sub>O-1Na<sub>2</sub>O-73SiO<sub>2</sub>, (C) 9B<sub>2</sub>O<sub>3</sub>-9Li<sub>2</sub>O-4Na<sub>2</sub>O-78SiO<sub>2</sub>, (D) 8B<sub>2</sub>O<sub>3</sub>-8Li<sub>2</sub>O-8Na<sub>2</sub>O-76SiO<sub>2</sub> and (E) 18B<sub>2</sub>O<sub>3</sub>-6Li<sub>2</sub>O-1Na<sub>2</sub>O-75SiO<sub>2</sub>.

<sup>b</sup> "Others" includes: BaO, Ce<sub>2</sub>O<sub>3</sub>, Cr<sub>2</sub>O<sub>3</sub>, CuO, K<sub>2</sub>O, La<sub>2</sub>O<sub>3</sub>, MgO, Nb<sub>2</sub>O<sub>5</sub>, NiO, PbO, SO<sub>4</sub>, ZnO and ZrO<sub>2</sub>.

Samples were prepared in 300 g batches using reagent-grade metal oxides, carbonates, H<sub>3</sub>BO<sub>3</sub>, and salts. The dry mixed batches were placed in Pt-alloy crucibles and melted at 1150-1200°C. After one hour, the molten glass was poured onto a clean, stainless steel plate. Approximately 25 g of each glass was heat-treated to simulate cooling along the centerline of a DWPF-type canister (ccc) to gauge the effects of thermal history on product performance.

Chemical compositions of each of the glasses were determined by Inductively Coupled Plasma-Atomic Emission Spectroscopy (ICP-AES) under the auspices of an analytical study plan. Each element was measured four times. Semi-quantitative X-ray diffraction (XRD) measurements were conducted on the ccc glasses with a scan rate of 0.04°2θ between 10 and 70°2θ, with a 4 s dwell time. Samples were prepared by mixing 5 wt% CaF<sub>2</sub> (internal standard) with approximately 1.5 to 2.5 g of glass. T<sub>L</sub> measurements were determined by a uniform temperature method, in which a glass sample is exposed to a constant temperature for a set period of time (e.g., 24± 2 hours) and then analyzed for crystals using optical microscopy. The Product Consistency Test (PCT) was performed in triplicate on each quenched and ccc glass to assess chemical durability using Method A of ASTM C1285-02 [9]. The resulting solutions were analyzed by ICP-AES under the auspices of an analytical study plan.

## RESULTS AND DISCUSSION

### Chemical Composition Measurements

In general, the measured compositions were consistent with the target compositions and the sums of oxides were within the interval 98-102 wt%. Scatter in the repeated measurements of Fe<sub>2</sub>O<sub>3</sub>, SiO<sub>2</sub> and NiO values was observed for some of the study glasses; none of which impact the outcome of this study. It is also of importance to note that the measured TiO<sub>2</sub> concentrations were consistent with the target compositions suggesting that TiO<sub>2</sub> retention (or solubility) up to approximately 3.5 wt% is not an issue within this compositional region for coupled operations.

### XRD

A summary of the types of crystals detected by XRD for each of the slow cooled (ccc) samples is

provided in Table III. Spinel formed in glasses that had a WL of at least 45%, while no crystals were detected in any of the glasses that had a WL of 40% or less (HWL-09, -12, -13 and HWL-15 through HWL-20). Optical microscopy of samples HWL-12 and HWL-13 confirmed that these samples were amorphous. Isolated spinel crystals were observed in samples HWL-9, -13 and -15, whereas crystals were found frequently in samples HWL-16, -17, -19 and -20 from sub-micron particles (HWL-17) to > 1 mm (HWL-19). Nepheline was detected in samples HWL-21 and HWL-22; however, this result was expected as nepheline was predicted by the DWPF Product Composition Control System.

Table III. XRD Phase Identification.

Glass ID	Sludge Type	XRD Phase Identification (ccc glass only)
HWL-01	Cluster 2 avg	Chromite (FeCr <sub>2</sub> O <sub>4</sub> )
HWL-02		Chromite (FeCr <sub>2</sub> O <sub>4</sub> )
HWL-03		Chromite (FeCr <sub>2</sub> O <sub>4</sub> )
HWL-04		Chromite (FeCr <sub>2</sub> O <sub>4</sub> )
HWL-05	Cluster 4 avg	Chromite (FeCr <sub>2</sub> O <sub>4</sub> )
HWL-06		Chromite (FeCr <sub>2</sub> O <sub>4</sub> )
HWL-07		Maghemite (Fe <sub>2</sub> O <sub>3</sub> )
HWL-08		Chromite (FeCr <sub>2</sub> O <sub>4</sub> )
HWL-09	MSP-001/SB8	Amorphous (no crystals detected)
HWL-10		Trevorite (NiFe <sub>2</sub> O <sub>4</sub> )
HWL-11		Chromite (FeCr <sub>2</sub> O <sub>4</sub> )
HWL-12		Amorphous (no crystals detected)
HWL-13		Amorphous (no crystals detected)
HWL-14		Magnetite (Fe <sub>3</sub> O <sub>4</sub> )
HWL-15	MSP-001/SB9	Amorphous (no crystals detected)
HWL-16		Amorphous (no crystals detected)
HWL-17		Amorphous (no crystals detected)
HWL-18		Amorphous (no crystals detected)
HWL-19		Amorphous (no crystals detected)
HWL-20		Amorphous (no crystals detected)
HWL-21	WOALD-SB19	Nepheline (NaAlSiO <sub>4</sub> ), Magnesium Iron Oxide (MgFe <sub>2</sub> O <sub>4</sub> )
HWL-22		Nepheline (NaAlSiO <sub>4</sub> ), Chromite (FeCr <sub>2</sub> O <sub>4</sub> )

Semi-quantitative analysis of the crystalline content was conducted for three samples (HWL-03, -06 and -22). Both HWL-03 and -06 contained approximately 6 wt% crystals, which was similar to the crystalline content of HWL-01, -02 and -04. HWL-22 had by far the highest crystalline content; approximately 35 wt% consisting mostly of nepheline. Examination of some of the other patterns suggested that HWL-05, -07, -10, -11 and -14 contained approximately 0.5-2.0 wt% crystals, and HWL-08 and HWL-21 contained approximately 3-4 wt% crystals after slow cooling.

### Liquidus Temperature

A summary of the predicted and measured  $T_L$  values is presented in Table IV along with any oxides that had concentrations outside of the model development ranges. To support

assessments of the applicability of the current  $T_L$  model to these compositional regions, one must first establish a baseline from which comparisons can be made. Brown et al. report a root mean squared error (RMSE) of approximately  $38^\circ\text{C}$  for the current model predictions [1]. The authors have used this estimated error ( $\pm 38^\circ\text{C}$ ) to gauge the applicability of the  $T_L$  model to the new glass compositional regions of interest. Fig. 1 shows the upper and lower 95% prediction intervals<sup>2</sup> (dashed lines) for the fitted model (solid line). The measured  $T_L$  values of several glasses are located above the upper limit of the prediction interval, which indicates that these values are significantly under-predicted by the model.

Table IV. Liquidus Temperatures for the Study Glasses.

Glass ID	Sludge Type	$T_L$ ( $^\circ\text{C}$ )		$\Delta T_L^a$ ( $^\circ\text{C}$ )	Compositional <sup>b</sup> Assessment Relative to Model Development Ranges
		Predicted	Measured		
HWL-01	Cluster 2 avg	1030	1152	122	Lower MgO
HWL-02		1071	1203	132	Lower MgO and SiO <sub>2</sub>
HWL-03		1046	1143	97	Lower MgO
HWL-04		1064	1193	129	Lower MgO and SiO <sub>2</sub>
HWL-05	Cluster 4 avg	1033	1143	110	Lower MgO
HWL-06		1072	1165	93	Lower MgO. Higher Fe <sub>2</sub> O <sub>3</sub> .
HWL-07		1010	1113	103	Lower MgO
HWL-08		1032	1152	120	Lower B <sub>2</sub> O <sub>3</sub> and MgO.
HWL-09	MSP-001/SB8	935	987	52	Lower MgO. Higher MnO and TiO <sub>2</sub> .
HWL-10		970	1031	61	
HWL-11		994	1086	92	Lower MgO. Higher MnO and TiO <sub>2</sub> .
HWL-12		837	957	120	Lower B <sub>2</sub> O <sub>3</sub> and MgO. Higher MnO and TiO <sub>2</sub> .
HWL-13		877	1023	146	
HWL-14		923	1086	163	Lower B <sub>2</sub> O <sub>3</sub> and MgO. Higher MnO and TiO <sub>2</sub> .
HWL-15	MSP-001/SB9	929	951	22	Lower MgO. Higher TiO <sub>2</sub> .
HWL-16		965	997	32	
HWL-17		1007	1030	23	
HWL-18		807	837	30	Lower MgO. Higher TiO <sub>2</sub> .
HWL-19		852	914	62	Lower MgO. Higher TiO <sub>2</sub> .
HWL-20		904	1029	125	Lower B <sub>2</sub> O <sub>3</sub> and MgO. Higher TiO <sub>2</sub> .

<sup>a</sup>  $\Delta T_L = \text{Measured } T_L - \text{Predicted } T_L$

<sup>b</sup> Assessment based on measured compositions.

<sup>2</sup> The upper and lower 95% prediction intervals were calculated by JMP™ Version 7.0.2, SAS Institute Inc., Cary, NC, 2008.

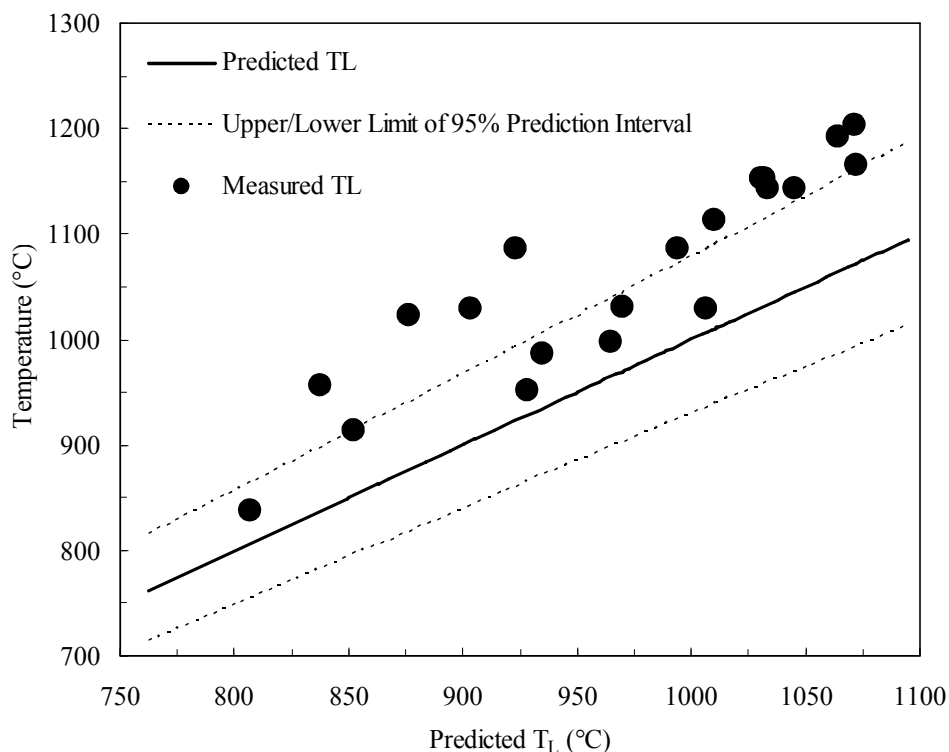


Fig. 1. A comparison of the measured T<sub>L</sub> values to the predicted T<sub>L</sub> values.

Relatively large discrepancies exist between the predicted and measured T<sub>L</sub> values for the cluster 2 and cluster 4 glass series compared to the RMSE for the model. The measured values for this series of glasses are consistently higher than the predicted values, which demonstrates that the current model under-predicts the T<sub>L</sub>s for both with and without Al-dissolution flowsheet glasses. With respect to overlap between the glass compositions and the model development ranges, each of the glasses has a lower MgO concentration than the model development range; however, MgO is not thought to be the cause of the considerable differences. The measured SiO<sub>2</sub> concentrations of HWL-02 and HWL-04 are lower than the model development ranges and could be the primary cause for the differences observed in these two glasses; however, these glasses were water quenched during the fabrication process and some of the larger fragments appeared to contain crystals, which may have caused the larger differences between the model predictions and measured values. For HWL-08, the B<sub>2</sub>O<sub>3</sub> measured concentration is outside of the model development ranges (but within the validation ranges as defined by Table I), which causes some concern over the applicability of the model in this specific compositional region for these combinations of oxides.

A review of the predicted versus measured T<sub>L</sub> values for the SB8 coupled operations with high B<sub>2</sub>O<sub>3</sub> content glasses (HWL-09 through HWL-11) indicates that the differences are higher for this series of glasses as compared to the series of SB9 with high B<sub>2</sub>O<sub>3</sub> content glasses. There appear to be larger differences between the predicted and measured T<sub>L</sub> values for HWL-12 through HWL-14, which are based on the lower B<sub>2</sub>O<sub>3</sub> concentration frit. On average, the differences for the SB8 based glasses are approximately 68°C and 143°C for the high and low B<sub>2</sub>O<sub>3</sub> concentrations, respectively. An evaluation of potential compositional differences between

the target SB8 glass compositional region as compared to the model development region does provide some insight into these larger differences. The measured concentrations of  $\text{TiO}_2$  and  $\text{MgO}$  are outside of the model development ranges; however, unlike the SB9 glasses, the  $\text{MnO}$  values for the SB8 glasses are also outside of the model development ranges. Each of the  $\text{MnO}$  target concentrations is greater than 3.4 wt% in glass as compared to the upper bound of 3.25 wt% in the model development ranges, which potentially leads to the larger differences for this series of glasses. In addition to  $\text{MnO}$ , the  $\text{B}_2\text{O}_3$  concentrations are beyond the model development ranges for HWL-11 and HWL-14. The larger difference exhibited by HWL-14 may be due to the presence of surface crystals on the quenched glass. As pointed out by Brown et al., the  $T_L$  model was validated with glasses whose compositions exceeded the model development ranges, but these data suggest that the combinations of the SB8 based glasses may be in a different glass compositional region (e.g., high  $\text{MnO}$ , low  $\text{B}_2\text{O}_3$ , and/or high  $\text{TiO}_2$  concentrations) [1]. The SB8 data are consistent with recent glass formulation efforts in support of the Cold Crucible Induction Melter (CCIM) demonstrations. The  $T_L$  of the Frit 202-A11 glass (targeting 50% WL) was predicted to be approximately 1130°C, but was measured to be approximately 1260°C [10]. A comparison of the target composition with the model development ranges indicated that the  $\text{B}_2\text{O}_3$ ,  $\text{Fe}_2\text{O}_3$ , and  $\text{MnO}$  contents were also outside of the  $T_L$  model development ranges.

There is considerably less difference between the predicted and measured  $T_L$  values for the series of SB9 coupled operations glasses based on the high  $\text{B}_2\text{O}_3$  content (18 wt%) frit (i.e., HWL-15, -16, and -17). A comparison of the model development and target glass compositional regions suggests complete overlap with the exception of the  $\text{TiO}_2$  and  $\text{MgO}$  concentrations. The  $\text{TiO}_2$  content is greater than the model development range, while the  $\text{MgO}$  content is below the model development range. These results indicate that not only are higher  $\text{TiO}_2$  concentrations possible with respect to retention or solubility, but that the  $T_L$  model is applicable in this compositional region. When comparing the measured  $T_L$  to the predicted  $T_L$  of the lower  $\text{B}_2\text{O}_3$  concentration SB9 glasses (8 wt%), the differences range from 30°C (HWL-18 targeting 32% WL) to 125°C (HWL-20 targeting 42%WL). In general, the data suggest that there is a shift in the compositional region (especially at the higher WLs) over which the applicability of the current  $T_L$  model becomes questionable. A comparison of the compositional overlap identifies only  $\text{TiO}_2$  and  $\text{MgO}$  differences between the model data and target glass compositional ranges for all glasses and a difference in the  $\text{B}_2\text{O}_3$  content of HWL-20. The compositional gaps for HWL-18 and HWL-19 (similar to those observed in HWL-15 through HWL-17) translate into  $T_L$  differences of 30 and 62°C, respectively. These differences are within or relatively close to the reported RMSE of 38°C for the current  $T_L$  model. The target  $\text{B}_2\text{O}_3$  content of HWL-20 is lower than the model development ranges, which could be the primary driver for the significant difference (125°C) between the measured and predicted  $T_L$  in that glass system. For the SB9 coupled operations study glasses, the  $T_L$  model appears to be very applicable for compositions that contain higher concentrations of  $\text{B}_2\text{O}_3$ . Larger differences are observed between the measured and predicted  $T_L$  values in glasses with a lower  $\text{B}_2\text{O}_3$  concentration. Although these glasses are within the model validation ranges, individual components or combinations of oxides being explored by these glasses are not in a region where the model has been validated. Thus, there is a need to generate additional data in these new compositional regions from which the  $T_L$  model coefficients could then be refined in order to more accurately predict  $T_L$  for glasses with combinations of oxides that are beyond those considered during model development and/or the



validation process.

### PCT

With respect to the durability of the study glasses, two glasses were of primary interest: HWL-21 and HWL-22. These two glasses target 50 and 55% WL, respectively, and were prone to nepheline formation based on the current discriminator value of 0.62 [11-13]. SRNL and PNNL have previously produced multiple glasses, which were prone to nepheline formation based on the 0.62 value, but did not yield nepheline upon slow cooling and showed no significant increase in PCT relative to their quenched counterparts. In fact, some of the glasses produced had discriminator values as low as 0.4 with  $\text{Al}_2\text{O}_3$  concentrations of  $\sim 26$  wt% [14]. These data indicated that the nepheline discriminator, although very effective at isolating glasses prone to nepheline formation, could be conservative leading to limitations in glass compositional regions that could improve waste loading (for high  $\text{Al}_2\text{O}_3$  concentration sludges) or melt rate. A key driver for suppressing nepheline formation in these glasses was the targeting of higher  $\text{B}_2\text{O}_3$  contents. Therefore, HWL-21 and HWL-22 were selected to provide more insight into the use of higher  $\text{B}_2\text{O}_3$  content to suppress nepheline formation. The normalized boron release (NL [B (g/L)]) results of the quenched versions of HWL-21 and HWL-22 were  $\sim 0.5$  to  $0.6$  g/L. These glasses are very durable after a rapid cooling schedule, which is consistent with previous data indicating that the formation of nepheline occurs upon slow cooling. When evaluating the PCT response of the ccc version of these two glasses, there is both a statistical and practical difference as compared to their quenched counterparts. The NL [B] values for these two glasses are approximately 4.7 and 90.0 g/L, respectively. The PCT response of HWL-21ccc is acceptable relative to the Environmental Assessment (EA) glass (16.695 g/L), whereas the NL [B] release of HWL-22 ccc exceeds the EA value by a factor of 5 [15]. These results are consistent with the semi-quantitative XRD analysis, in which the crystalline content increased from approximately 3-4 wt% to 35 wt% after slow cooling. Based on PCT response these glasses it appears that increasing the  $\text{B}_2\text{O}_3$  concentration in glass does not consistently suppress the formation of nepheline in glasses with higher  $\text{Al}_2\text{O}_3$  and/or  $\text{Na}_2\text{O}$  content.

All of the other study glasses (both radioactive and non-radioactive) were very acceptable relative to the EA glass benchmark with NL [B] releases ranging from 0.5 to 1.1 g/L for the quenched glasses and 0.4 to 0.9 g/L for the ccc versions. This is not surprising given that the selection of glasses for HWL-01 through HWL-20 were primarily chosen in order to gain insight into  $T_L$  issues and were not intended to challenge durability.

### CONCLUSIONS

$\text{TiO}_2$  concentrations up to  $\sim 3.5$  wt% were retained in DWPF type glasses, where retention is defined as the absence of crystalline  $\text{TiO}_2$  (undissolved or unreacted) in the as-fabricated glasses. Although this  $\text{TiO}_2$  content does not bound the projected SWPF high output flowsheet (up to 6 wt%  $\text{TiO}_2$  may be required in glass), these data indicate the potential for increasing the  $\text{TiO}_2$  limit in glass from the current limit in PCCS of 2 wt% (based strictly on retention or solubility).

For those study glasses which had very close compositional overlap with the model development and/or model validation ranges (except  $\text{TiO}_2$  and  $\text{MgO}$  concentrations), there was very little difference in the predicted and measured  $T_L$  values, even though the  $\text{TiO}_2$  contents were above the 2 wt% upper limit. The results indicate that the current  $T_L$  model is applicable in these

compositional regions. As the compositional overlap between the model validation ranges diverged from the target glass compositions, the  $T_L$  data suggest that the model significantly under-predicted the measured values by as much as 163°C. These discrepancies imply that there are individual oxides or their combinations that were outside of the model development and/or validation range over which the model was previously assessed. These oxides include  $B_2O_3$ ,  $SiO_2$ ,  $MnO$ ,  $TiO_2$  and/or their combinations. More data would be required to fill in these anticipated DWPF compositional regions so that the model coefficients could be refit to account for these differences.

Based on the PCT responses of HWL-21 and HWL-22 (two glasses that were prone to nepheline formation) it appears that increased  $B_2O_3$  concentration in glass does not consistently suppress the formation of nepheline in glasses with higher  $Al_2O_3$  and/or  $Na_2O$  content. Although the quenched versions of these glasses were very acceptable, the ccc glasses exhibited a considerable decrease in durability. In fact, one of the glasses had a release that was 5 times greater than the EA benchmark glass. These results suggest a need for a more fundamental understanding of the compositional and kinetic effects of nepheline formation in high WL glasses.

## REFERENCES

1. K.G. Brown, C.M. Jantzen, and G. Ritzhaupt, "Relating Liquidus Temperature to Composition for Defense Waste Processing Facility (DWPF) Process Control," Westinghouse Savannah River Company, Aiken, SC, WSRC-TR-2001-00520, Revision 0, 2001.
2. T.B. Edwards, D.K. Peeler, and S.L. Marra, "Revisiting the Prediction Limits for Acceptable Durability," Westinghouse Savannah River Company, Aiken, SC, WSRC-TR-2003-00510, Revision 0, 2003.
3. F.C. Raszewski, T.B. Edwards, and D.K. Peeler, "Enhanced DOE High-Level Waste Melter Throughput Studies: Glass Selection Strategy," Savannah River National Laboratory, Aiken, SC, WSRC-STI-2007-00652, Rev. 0, 2007.
4. C.M. Jantzen and J.C. Marra, "High Level Waste (HLW) Vitrification Experience in the Us: Application of Glass Product/Process Control to Other HLW and Hazardous Wastes," Savannah River National Laboratory, Aiken, SC, WSRC-STI-2007-00238, 2007.
5. J.D. Newell, T.B. Edwards, and D.K. Peeler, "Initial MAR Assessments to Assess the Impact of Al-Dissolution on DWPF Operating Windows," Savannah River National Laboratory, Aiken, SC, WSRC-STI-2007-00688, Rev. 0, 2007.
6. D.K. Peeler, M.E. Smith, M.E. Stone, T.B. Edwards, and J.D. Newell, "Frit Development for High  $Al_2O_3$  Based Sludges: Task Technical and Quality Assurance Plan," Savannah River National Laboratory, Aiken, SC, WSRC-STI-2007-00504, Rev. 0, 2007.
7. D.K. Peeler and T.B. Edwards, "High-Level Review of the Impacts of CST and RF on DWPF Processing: A Glass Formulation Perspective " Savannah River National Laboratory, Aiken, SC, SRNL-PSE-2007-00177, 2007.
8. D.P. Chew, M.J. Mahoney, and J.R. Vitali, "Life-Cycle Liquid Waste Disposition System Plan - Revision 14," Washington Savannah River Company, Aiken, SC, LWO-PIT-2007-00062, 2007.

9. “Standard Test Methods for Determining Chemical Durability of Nuclear, Hazardous, and Mixed Waste Glasses and Multiphase Glass Ceramics: The Product Consistency Test (PCT),” ASTM International, West Conshohocken, PA, ASTM C 1285-02(2008), 2008.
10. D.K. Peeler, K.M. Fox, T.B. Edwards, D.R. Best, I.A. Reamer, and R.J. Workman, “Data Packet for the Frit 202-A11 - SB3 Glass System: A Candidate for the Cold Crucible Induction Melter (CCIM) Demonstration,” Savannah River National Laboratory, Aiken, SC, WSRC-STI-2007-00302, 2007.
11. T.B. Edwards, D.K. Peeler, and K.M. Fox, “The Nepheline Discriminator: Justification and DWPF PCCS Implementation Details,” Washington Savannah River Company, Aiken, SC, WSRC-STI-2006-00014, Revision 0, 2006.
12. H. Li, J.D. Vienna, P. Hrma, D.E. Smith, and M.J. Schweiger, “Nepheline Precipitation in High-Level Waste Glasses: Compositional Effects and Impact on the Waste Form Acceptability,” *Proc. Mat. Res. Soc.*, **465** 261-8 (1997).
13. T.J. Menkhaus, P. Hrma, and H. Li, “Kinetics of Nepheline Crystallization from High-Level Waste Glass,” *Ceram. Trans.*, **107** 461-8 (2000).
14. K.M. Fox and D.K. Peeler, “Demonstration of Very High Aluminum Retention in Simulated HLW Glass,” Savannah River National Laboratory, Aiken, SC, SRNL-PSE-2007-00231 Rev. 0, 2007.
15. C.M. Jantzen, N.E. Bibler, D.C. Beam, C.L. Crawford, and M.A. Pickett, “Characterization of the Defense Waste Processing Facility (DWPF) Environmental Assessment (EA) Glass Standard Reference Material,” Westinghouse Savannah River Company, Aiken, SC, WSRC-TR-92-346, Rev. 1, 1993.